



IJRASET

International Journal For Research in
Applied Science and Engineering Technology



INTERNATIONAL JOURNAL FOR RESEARCH

IN APPLIED SCIENCE & ENGINEERING TECHNOLOGY

Volume: 8 Issue: VIII Month of publication: August 2020

DOI: <https://doi.org/10.22214/ijraset.2020.31084>

www.ijraset.com

Call:  08813907089

E-mail ID: ijraset@gmail.com

Experimental Investigation of Performance on Vapour Absorption Refrigeration System using Solar Collector

Mohan Prasath P R¹, Dr. Velliangiri M², Aswath A S³, Prakash M⁴, Chandrakumar S⁵

^{1, 3, 4, 5}Undergraduate students, ²Assistant professor, Department of Mechanical Engineering, Coimbatore Institute of Technology, Coimbatore – 641014, Tamil Nadu, India

Abstract: Solar energy is the most abundant source of energy in India and we don't have efficient technology to tap this energy source and use it for varied applications. The primary focus of this paper is utilizing solar energy for designing and studying of environmental friendly vapour absorption refrigeration system. The vapour absorption system is two fluid systems comprising of ammonia and water and it has three phases: Evaporation, Absorption, and Regeneration. Here in this Refrigeration system when low boiling point refrigerant evaporate, it takes some heat away with it providing the cooling effect and changes the gas back into liquid. In this system compressor is replaced by Generator and Absorber. The experiment is done with the replacement of heat exchanger powered by the hot water from the solar collector in the place of generator.

Keywords: Solar, phases, generator, absorber

I. INTRODUCTION

Solar energy is the primary source of energy and it drives the day to day life. Nearly most part of the earth acquires adequate amount of solar energy. The harvesting of solar energy is also comparatively easy and cost efficient process. A refrigeration system utilizes work supplied by an electric motor to transfer heat from a space to be cooled to a high temperature sink (place to be heated). While comparing the advantages and disadvantages of various cooling systems, there are two most important parameters namely operating temperature and the coefficient of performance. Considering these two major factors we have to use solar heater as a work input as a purpose of increasing the COP level. Solar vapour absorption refrigerators resolve the basic needs in the remote village where the electricity is not available. Solar energy is a very large, inexhaustible source of energy. The power from the sun intercepted by the earth is approximately 1.8×10^{11} MW which is much larger than the present consumption rate on the earth of all commercial energy sources. Thus, solar energy could supply all the present and future energy needs of the world on the continuing basis.

II. METHODOLOGY

The sequence of works carried out is depicted in the following flowchart which clearly indicates the methodology that is been followed.

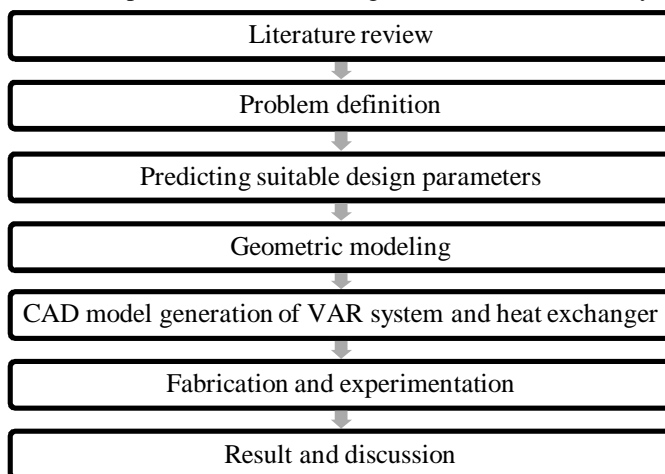


Fig. 1 Methodology

III.LITERATURE REVIEW

Sen et al. (2016) experimentally studied and numerically analyzed dependency on non renewable energy resources for electricity production. There is need to develop a refrigeration system which is either independent of non renewable energy or requires a very little amount of the same. So this problem attracted the researcher towards development of the vapour absorption system, because it is environment and eco friendly and can use low grade energy such as solar energy, waste energy etc. Besides many advantages the absorption system has coefficient of performance less than unity. To be served by its advantages efficiently, in recent years, research has been devoted to improvement of the performance of vapour absorption system. The authors discussed a number of researches on working fluid.

Ganguly et al. (2019) experimentally studied and numerically analysed the provision of increasing the heat storage in a SGSP by increasing the thermal mass of it. It also addresses the method of enhancing the thermal performance of a SGSP by increasing the thermal mass, while adding heat from external sources. Earlier studies have proved that adding external heat to the SGSP for storage enhances the thermal performance of it significantly. This study aims to prove that increasing the thermal mass of storage further increases the energy efficiency of a SGSP when external heat is added to it. A hybrid system of a SGSP coupled with evacuated tube solar collectors is used in this study. Several parameters like storage temperature in LCZ, heat addition flux and heat addition efficiency of ETSC, instantaneous efficiency of SGSP, heat extraction from SGSP are studied in this paper for different cases of with and without heat addition and with normal and enhanced thermal mass. The authors found that increasing thermal mass can significantly enhance the thermal performance and efficiency of a SGSP.

Chen et al. (2013) experimentally studied and numerically analysed a new type of absorption refrigeration cycle that is co-driven both by solar energy and electricity was evaluated. The principle of a heat transformer was applied to the absorption refrigeration system to increase its efficiency. In this paper, a thermodynamic model describing the performance of the new cycle was developed and a computer program was written to evaluate its performance. The COP, condenser heat load, the theoretical minimum evaporating temperature and refrigeration capacity for a typical daily load of the system were calculated and compared with those of traditional absorption refrigeration systems. The results of the authors show that the new cycle not only overcomes some shortcomings of the traditional absorption cycle with unsteady energy input from a variable source such as solar energy, but also increases the system's coefficient of performance.

Umap et al. (2017) experimentally studied and numerically analysed input for vapor absorption system is in the form of heat hence these systems are also called as thermal operated systems. Since the liquids are used to absorb the refrigerants, they also called as wet absorption system. The authors work was to check the performance like COP and circulation ratio using solar based system to observe the variables like flow rate and composition.

Xinyu et al. experimentally studied and numerically analysed the higher coefficient of thermal performance for water-in glass evacuated tube solar water heater in china. In this test, the performance of more than 1000 water-in-glass evacuated tube SWHs according to Chinese standards and found that the heat loss from the storage tank and capacity of the solar collector affected their thermal performance. In this study, they found that a shorter evacuated tube exhibited better thermal performance than longer tube. A shorter tube is also less likely to be damaged during transportation. The experimental results obtained by authors showed that the distance between the centers of the tubes will have an effect on the thermal performance of a water-in-glass evacuated solar water heater without diffuse reflectors.

IV.EXPERIMENTAL METHODOLOGY

The experimentation process has dealt with by following certain sequence of works which is depicted in the following flowchart.

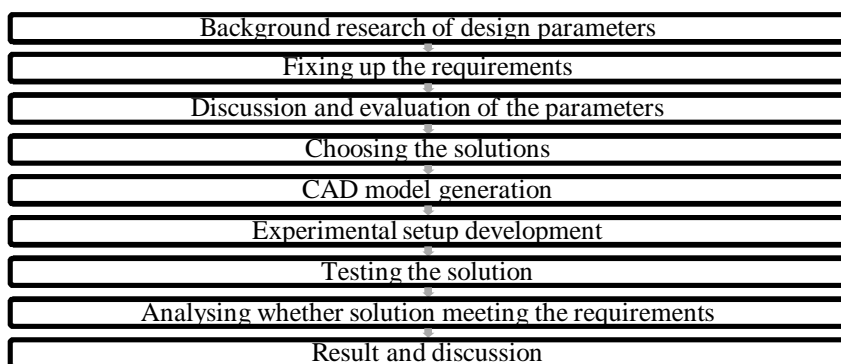


Fig. 2 Experimentation methodology

V. EXPERIMENTAL SETUP

Experimental setup describes how the experimentation was done and summarizes the data taken. This section contains the instruments used, detectors used and the procedure followed to collect the data. Experiments are conducted to be able to predict phenomenon. The experiments were conducted in the fabricated experimental setup. Material used in the experimental setup is stainless steel. Stainless steel is a family of iron-based alloys that contain a minimum of approximately 11% chromium, a composition that prevents the iron from rusting, as well as providing heat resistant properties. Different types of stainless steel include the elements carbon (from 0.03% to greater than 1.00%), nitrogen, aluminium, silicon, sulphur, titanium, nickel, copper, selenium, niobium, and molybdenum. Resistance to corrosion and staining, low maintenance, and familiar lustre make stainless steel an ideal material for many applications where both the strength and corrosion resistance are required. The components are evaporator, condenser, generator, absorber, pump, heat exchanger, expansion devices and solar collector. The experimental setup is schematically represented as follows:

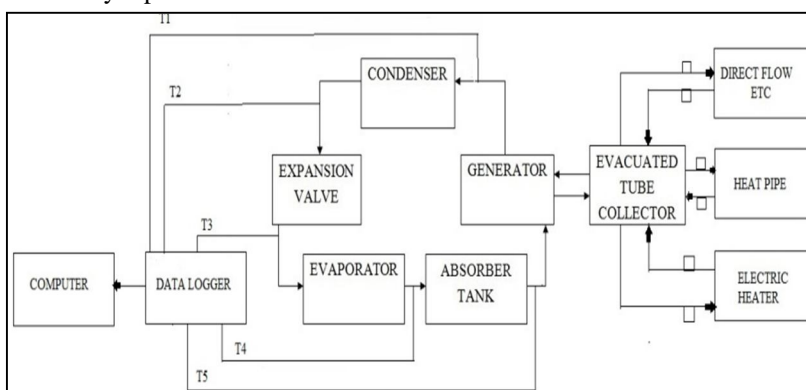


Fig. 3 Experimental setup

VI. GOVERNING EQUATIONS

Major equations used to evaluate COP of the system are as follows [14]. Various properties at salient points are denoted as suffice as per numbers given.

The mass balance of strong solution, weak solution and refrigerant can be written as

$$m_r \square m_w \square m_s \square 0 \tag{1}$$

The specific rich solution circulation f can be written as

$$f = \begin{cases} x_9 - x_4 \\ x_3 - x_4 \end{cases} \tag{2}$$

The strong and weak solution flow rates are given by equations (3) and (4) respectively

$$m_s \square m_r \square f \tag{3}$$

$$m_w \square m_r \square \square f \square 1 \square \tag{4}$$

Energy balance of different components of absorption refrigeration system can be written by equations (5) to (13)

$$Q_e \square m_r \square \square h_{13} \square h_{12} \square \tag{5}$$

Heat added in the generator can be written as

$$Q_g \square m_r \square \square h_7 \square h_4 \square f \square \square h_4 \square h_3 \square \square \tag{6}$$

Pump work can be written as

$$w_p \square m_r \square f \square v_1 \square \square P_2 \square P_1 \square \square \square \square \square \tag{7}$$

Heat rejected in the condenser can be written as

$$Q_c \square m_r \square \square h_9 \square h_{10} \square \square \square \tag{8}$$

Heat rejected in the absorber can be written as

$$Q_a \square m_r \square \square h_{14} \square h_6 \square f \square \square h_6 \square h_1 \square \square \tag{9}$$

Heat transfer in solution heat exchanger can be written as

$$Q_{SHE} \square m_r \square \square \square f \square 1 \square \square \square h_4 \square h_5 \square \tag{10}$$

Heat transfer in refrigerant heat exchanger can be written as

$$Q_{RHE} \square m_r \square \square h_{10} \square h_{11} \square \square \square \square \tag{11}$$

Coefficient of performance of the absorption refrigeration system can be written as

$$\frac{Q_e}{Q_g + W_p} \tag{12}$$

Second law or exergetic efficiency of the absorption refrigeration system can be written as

$$\eta_{exe} = \frac{-Q_e \times \left(1 - \frac{T_0}{T_e}\right)}{\left(Q_g \times \left(1 - \frac{T_0}{T_g}\right)\right) + W_p} \tag{13}$$

VII. OPTIMISATION FOR COP AND EXERGETIC EFFICIENCY

COP and exergetic efficiency mainly depends on six parameters i.e. condenser temperature, absorber temperature, evaporator temperature, generator temperature, solution heat exchanger effectiveness, and refrigerant heat exchanger effectiveness of absorption refrigeration system. In present study condenser and absorber temperatures are considered as same. Therefore, total five parameters are considered as independent variables. All 1024 possible combinations of five independent variables are developed based on selected range of each parameter as shown in Table 1. All parameters are selected in ascending order to make all possible combinations. Condenser temperatures are selected for the possible Indian weather conditions. Evaporator temperatures are chosen for air conditioning and cold storage applications. Generator temperature and effectiveness of refrigerant and absorber heat exchanger range are selected based on the literature.

TABLE I
Factors and Their Levels

Factors	Level 1	Level 2	Level 3	Level 4
Condenser temperature, T_c (°C)	35	40	45	50
Evaporator temperature, T_e (°C)	-5	0	5	10
Generator temperature, T_g (°C)	120	130	140	150
Effectiveness of refrigerant heat exchanger, ϵ_{RHE}	0.6	0.65	0.7	0.75
Effectiveness of solution heat exchanger, ϵ_{SHE}	0.6	0.65	0.7	0.75

Taguchi method is commonly adopted for optimizing design parameters. Taguchi method of design of experiment (DOE) is used to make statistical analysis of all independence variables. Four levels and five factors Taguchi design is used as given in Table 2 and sixteen different combinations are obtained based on L16 orthogonal array.

TABLE II
Taguchi Design

1	1	1	1	1
1	2	2	2	2
1	3	3	3	3
1	4	4	4	4
2	1	2	3	4
2	2	1	4	3
2	3	4	1	2
2	4	3	2	1
3	2	4	3	1
3	3	1	2	4
3	4	2	1	3
4	1	4	2	3
4	2	3	1	4
4	3	2	4	1
4	4	1	3	2

Based on Taguchi design, sixteen different combinations of five different independent variables are developed as per Table 3. With the help of EES software, COP and exergetic efficiency are evaluated for all sixteen combination.

TABLE III
Results of COP and Exergetic Efficiency for Taguchi Design

T_c (°C)	T_e (°C)	T_g (°C)	ϵ_{RHE}	ϵ_{SHE}	COP	η_{exe} (%)
35	-5	120	0.6	0.6	0.4825	23.94
35	0	130	0.65	0.65	0.5527	21.15
35	5	140	0.7	0.7	0.6052	17.36
35	10	150	0.75	0.75	0.6500	13.34
40	-5	130	0.7	0.75	0.4904	22.44
40	0	120	0.75	0.7	0.5079	20.74
40	5	150	0.6	0.65	0.5495	14.82
40	10	140	0.65	0.6	0.5787	12.59
45	-5	140	0.75	0.65	0.4084	17.45
45	0	150	0.7	0.6	0.4564	15.31
45	5	120	0.65	0.75	0.5070	16.44
45	10	130	0.6	0.7	0.5554	12.83
50	-5	150	0.65	0.7	0.3743	14.99
50	0	140	0.6	0.75	0.4186	14.68
50	5	130	0.75	0.6	0.3950	11.86
50	10	120	0.7	0.65	0.4390	10.72

Taguchi method uses a statistical measure of performance, which is called signal-to-noise (SN) ratio. SN ratio helps in data analysis and prediction of optimum results. Simulation results are transferred in to SN ratio. SN ratio response determines the control parameters such as T_c , T_e , T_g , ϵ_{RHE} , and ϵ_{SHE} on COP and exergetic efficiency. MINITAB is used for the parameter settings with the highest SN ratio, which always produces the optimum quality with lower variance. Highest values of COP and exergetic efficiency are desirable. Therefore, ‘Larger is the better’ type category of the performance characteristic for COP and exergetic efficiency are selected to analyse the SN ratio as shown in Table 4 and 5.

TABLE IV
SN RATION FOR COP

T_c (°C)	T_e (°C)	T_g (°C)	ϵ_{RHE}	ϵ_{SHE}	COP	SN
35	-5	120	0.6	0.6	0.4825	-6.3301
35	0	130	0.65	0.65	0.5527	-5.1502
35	5	140	0.7	0.7	0.6052	-4.362
35	10	150	0.75	0.75	0.6500	-3.7417
40	-5	130	0.7	0.75	0.4904	-6.189
40	0	120	0.75	0.7	0.5079	-5.8844
40	5	150	0.6	0.65	0.5495	-5.2006
40	10	140	0.65	0.6	0.5787	-4.7509
45	-5	140	0.75	0.65	0.4084	-7.7783
45	0	150	0.7	0.6	0.4564	-6.8131
45	5	120	0.65	0.75	0.5070	-5.8998
45	10	130	0.6	0.7	0.5554	-5.1079
50	-5	150	0.65	0.7	0.3743	-8.5356
50	0	140	0.6	0.75	0.4186	-7.564
50	5	130	0.75	0.6	0.3950	-8.0681
50	10	120	0.7	0.65	0.4390	-7.1507

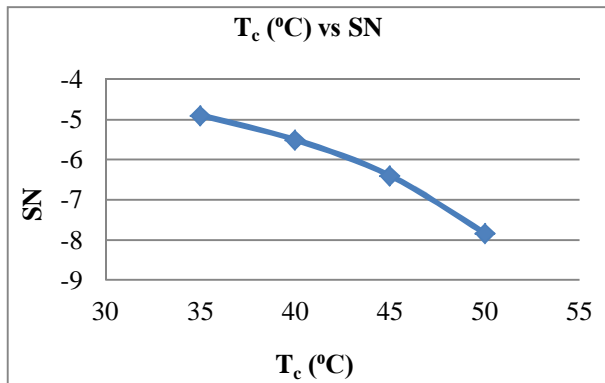


Fig. 4 Variation of SN with T_c

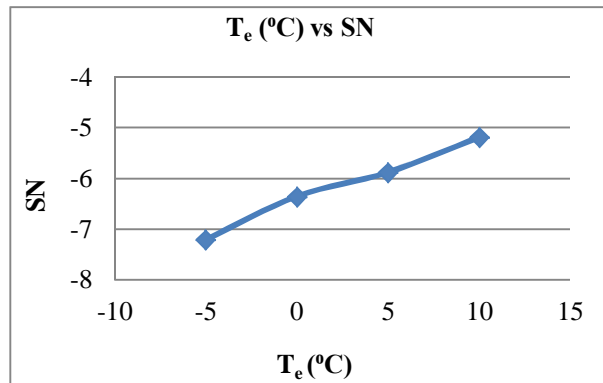


Fig. 5 Variation of SN with T_e

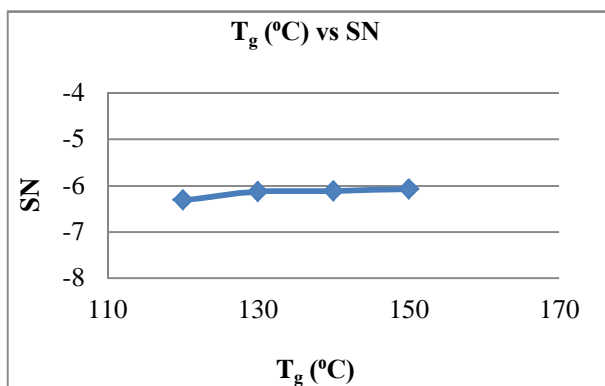


Fig. 6 Variation of SN with T_g

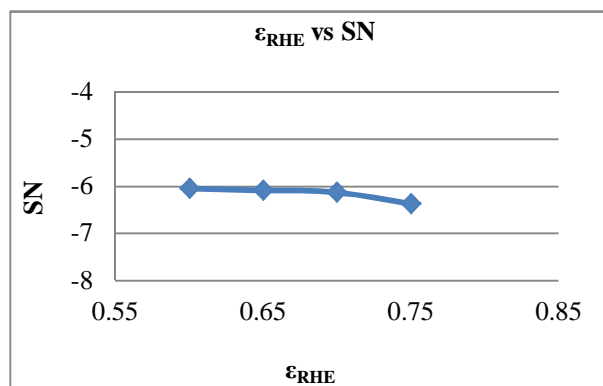


Fig. 7 Variation of SN with ϵ_{RHE}

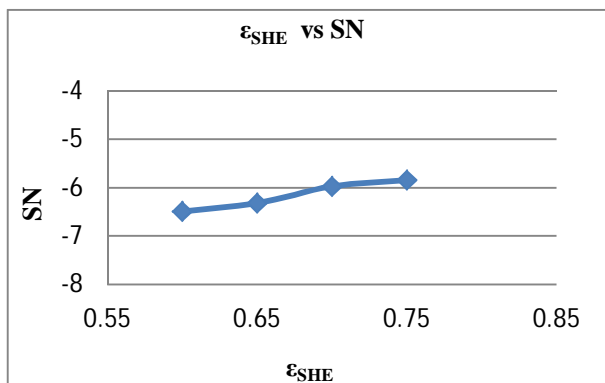


Fig. 8 Variation of SN with ϵ_{SHE}

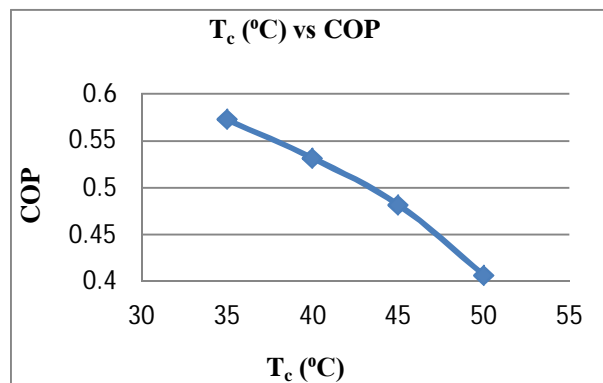


Fig. 9 Variation of COP with T_c

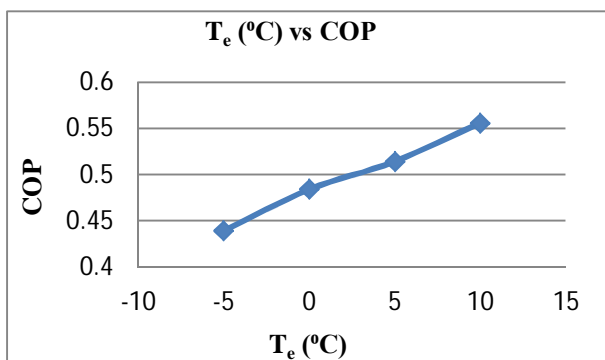


Fig. 10 Variation of COP with T_e

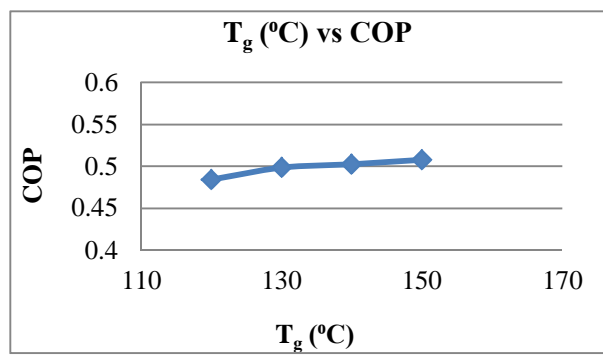


Fig. 11 Variation of COP with T_g

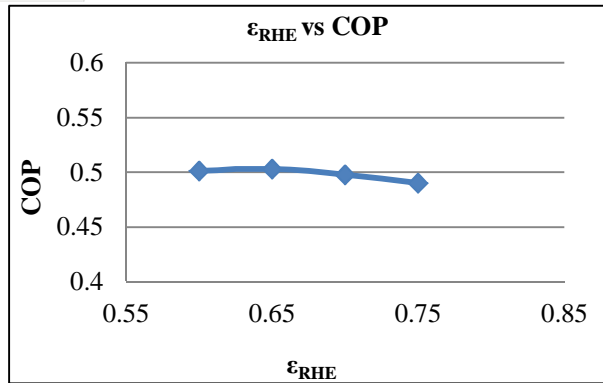


Fig. 12 Variation of COP with ϵ_{RHE}

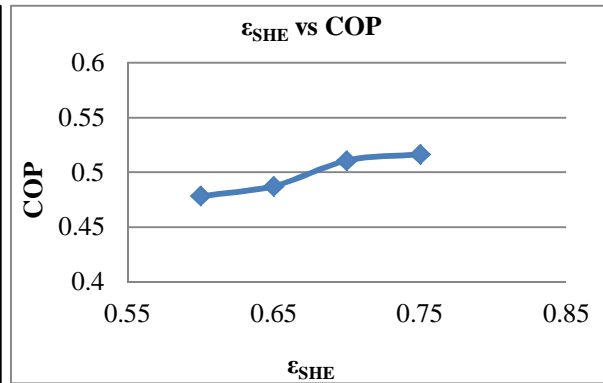


Fig. 13 Variation of COP with ϵ_{SHE}

Fig 4 – Fig 8 and Fig 9 – Fig 13 shows the main effect plot of mean of SN ratio and mean of means for COP respectively. It is observed that $T_c = 35^\circ\text{C}$, $T_e = 10^\circ\text{C}$, $T_g = 150^\circ\text{C}$, $\epsilon_{RHE} = 0.6$ and $\epsilon_{SHE} = 0.75$ and $T_c = 35^\circ\text{C}$, $T_e = 10^\circ\text{C}$, $T_g = 150^\circ\text{C}$, $\epsilon_{RHE} = 0.65$ and $\epsilon_{SHE} = 0.75$ are suitable parameters for maximum COP. From predicted values of Taguchi analysis, COP is 0.6612 for mean value of $T_c = 35^\circ\text{C}$, $T_e = 10^\circ\text{C}$, $T_g = 150^\circ\text{C}$, $\epsilon_{RHE} = 0.6$, and $\epsilon_{SHE} = 0.75$.

TABLE V
SN Ration for EXERGETIC Efficiency

T_c ($^\circ\text{C}$)	T_e ($^\circ\text{C}$)	T_g ($^\circ\text{C}$)	ϵ_{RHE}	ϵ_{SHE}	η_{exe} (%)	SN
35	-5	120	0.6	0.6	23.94	27.5825
35	0	130	0.65	0.65	21.15	26.5062
35	5	140	0.7	0.7	17.36	24.791
35	10	150	0.75	0.75	13.34	22.5031
40	-5	130	0.7	0.75	22.44	27.0205
40	0	120	0.75	0.7	20.74	26.3362
40	5	150	0.6	0.65	14.82	23.417
40	10	140	0.65	0.6	12.59	22.0005
45	-5	140	0.75	0.65	17.45	24.8359
45	0	150	0.7	0.6	15.31	23.6995
45	5	120	0.65	0.75	16.44	24.318
45	10	130	0.6	0.7	12.83	22.1645
50	-5	150	0.65	0.7	14.99	23.516
50	0	140	0.6	0.75	14.68	23.3345
50	5	130	0.75	0.6	11.86	21.4817
50	10	120	0.7	0.65	10.72	20.6039

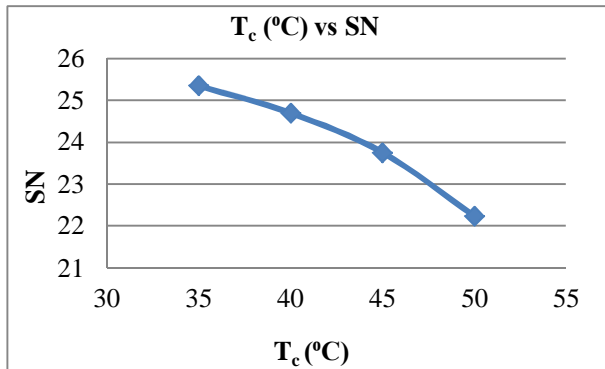


Fig. 14 Variation of SN with T_c

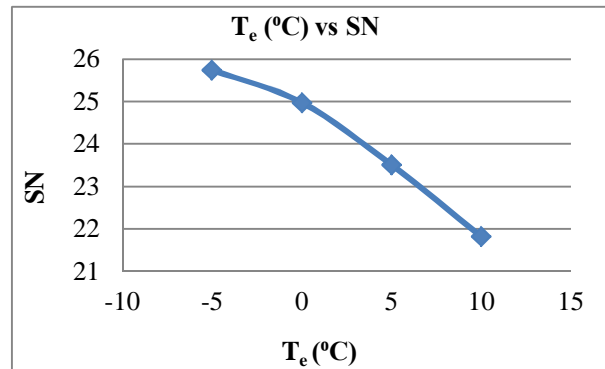


Fig. 15 Variation of SN with T_e

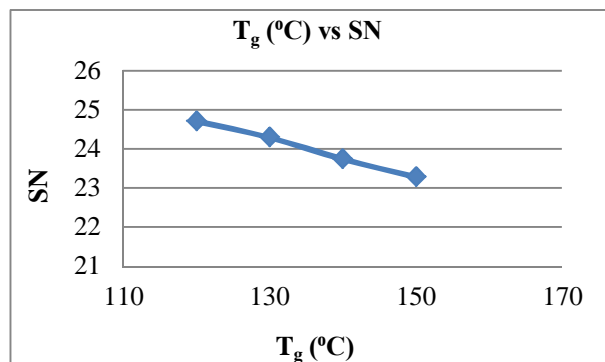


Fig. 16 Variation of SN with T_g

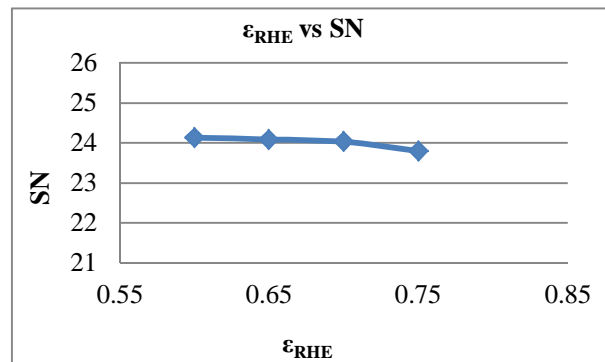


Fig. 17 Variation of SN with ϵ_{RHE}

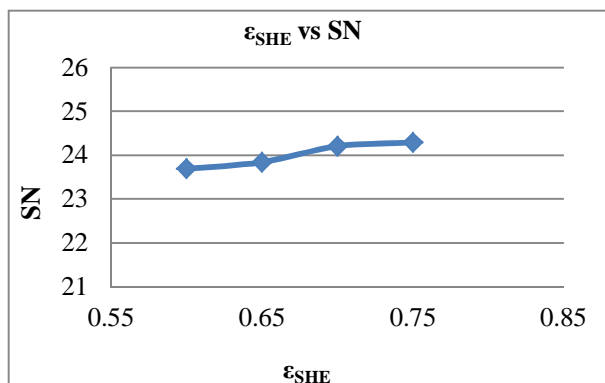


Fig. 18 Variation of SN with ϵ_{SHE}

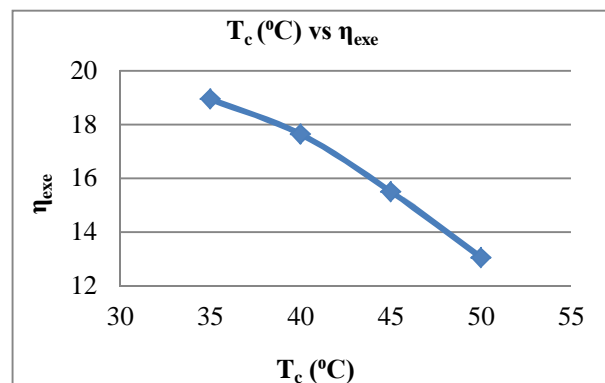


Fig. 19 Variation of η_{exe} with T_c

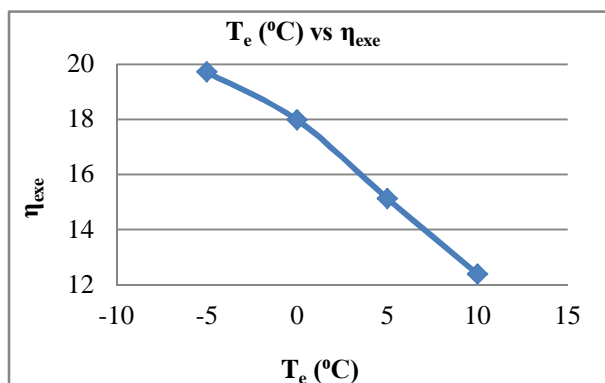


Fig. 20 Variation of η_{exe} with T_e

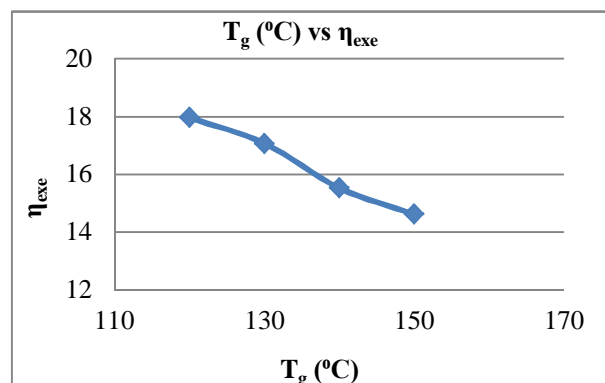


Fig. 21 Variation of η_{exe} with T_g

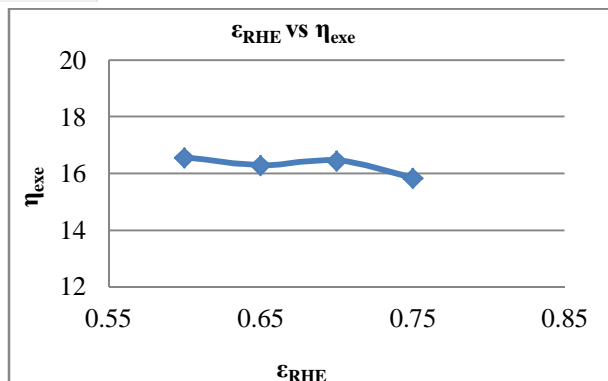


Fig. 22 Variation of η_{exe} with ϵ_{RHE}

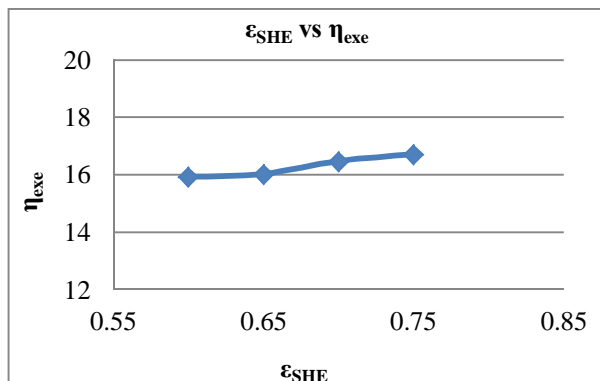


Fig. 23 Variation of η_{exe} with ϵ_{SHE}

Fig. 14 – Fig 18 and Fig 19 – Fig 23 shows the main effect plot of mean of SN ratio and mean of means for exergetic efficiency respectively. From both the plots it is observed that $T_c = 35^\circ\text{C}$, $T_e = -5^\circ\text{C}$, $T_g = 120^\circ\text{C}$, $\epsilon_{RHE} = 0.6$ and $\epsilon_{SHE} = 0.75$ are suitable parameters for maximum exergetic efficiency. From predicted values of Taguchi analysis, prediction for exergetic efficiency is 24.74% for mean value of $T_c = 35^\circ\text{C}$, $T_e = -5^\circ\text{C}$, $T_g = 120^\circ\text{C}$, $\epsilon_{RHE} = 0.6$ and $\epsilon_{SHE} = 0.75$.

VIII. CFD ANALYSIS

The analysis is carried out in ANSYS 18.1 using fluid fluent CFD for meshing. Simulations are carried out using ANSYS Fluent, a finite volume solver. After opening ANSYS Workbench, the type of Analysis is chosen to be CFD Fluent.

The geometry to be analysed is then need to imported from CAD platform. The sequence by which the geometry is imported as follows:

Workbench > Geometry > File > Import external Geometry file > CAD model

After importing the CAD model, meshing or grid generation is carried out. At the setup portion Solver type was selected as pressure based and time was transient. The gravity value of Y is chosen to be -9.81m/s^2 . The model is chosen to be multiphase model and the number of Eulerian phases is chosen to be 3 namely Air (primary phase), Ammonia liquid (secondary phase) and Ammonia vapour (secondary phase). The formulation is chosen to be implicit and the mass transfer mechanism is chosen to be Evaporation – Condensation.

The solver settings are mentioned in the form of table mentioned below.

TABLE VI
Analysis Setup and Initialization Values

S. No	SOLVER SETTINGS	
1.	Solver type	Pressure based
2.	Time	Transient
3.	Gravity	$Y = -9.81 \text{ m/s}^2$
4.	Models	Multiphase : Volume of fluid Number of Eulerian phases: 3 Volume fraction parameters: ✓ Formulation: Implicit ✓ Body force formulation: Implicit body force
5.	Phases	✓ Air: Primary phase ✓ Ammonia liquid: Secondary phase ✓ Ammonia vapour: Secondary phase
6.	Interactions (Mass)	✓ Number of mass transfer mechanisms: One ✓ From phase: Ammonia liquid ✓ To phase: Ammonia vapour ✓ Mechanism: Evaporation - Condensation ✓ Saturation temperature: 239.81 K

7.	Interactions (Surface tension)	<ul style="list-style-type: none"> ✓ Surface tension coefficient: 0.02 N/m (Ammonia liquid)
8.	Boundary conditions	<p>Inlet conditions:</p> <ul style="list-style-type: none"> ✓ Velocity inlet is chosen ✓ Velocity magnitude: 1 m/s² ✓ Temperature: 229.81 K <p>Outlet conditions:</p> <ul style="list-style-type: none"> ✓ Pressure outlet is chosen ✓ Outlet gauge pressure: 0 Pa ✓ Backflow total temperature: 300 K <p>Wall:</p> <ul style="list-style-type: none"> ✓ Type: Wall ✓ Temperature: 273.15 K
S. No	INITIALIZATION	
1.	Solution initialization	Hybrid initialization
2.	Run calculation	<ul style="list-style-type: none"> ✓ Time step size: 1 ✓ Number of time steps: 50 ✓ Maximum iterations per time step: 20

IX. RESULTS AND DISCUSSIONS

The results are extracted from CFD POST after the analysis from fluent flow solver. The different contours of condenser are displayed below.

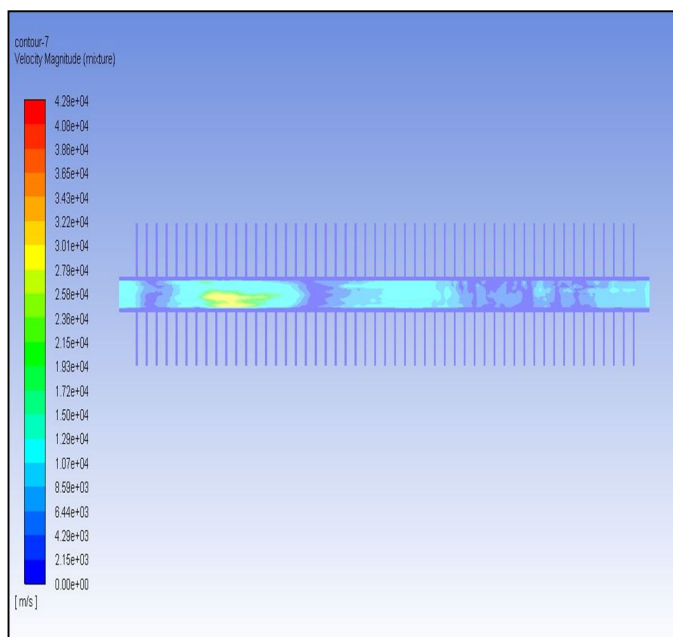


Fig. 24 Velocity magnitude contour of condenser

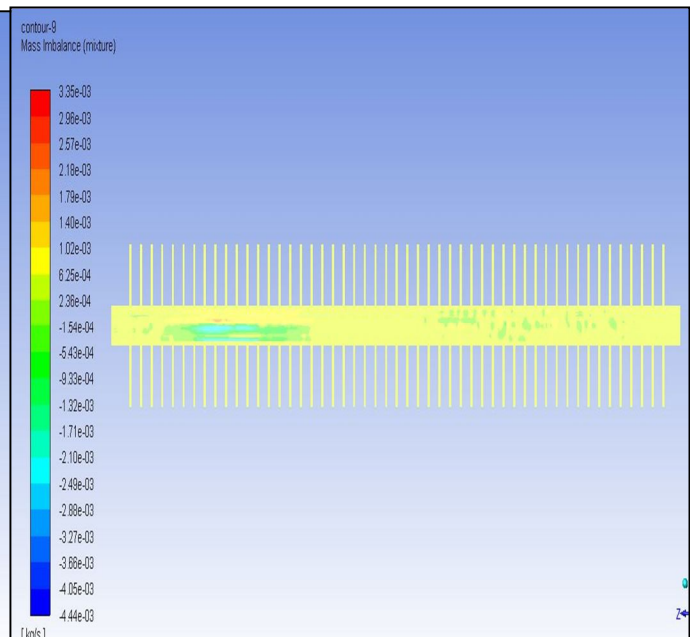


Fig. 25 Mass imbalance contour of condenser

The velocity magnitude at the inlet is given to be 1 m/s². Based on the phases it passes through, the velocity magnitude is inconsistent and after passing through the three stages, it is seen that the velocity magnitude is uniform at the exhaust of the condenser.

The mass balance contour of condenser is depicted above. The mass imbalance is found to be constant throughout the condenser except in regions where there is a phase change. After passing through the three phases, it is inferred that the mass imbalance is found to be constant throughout.

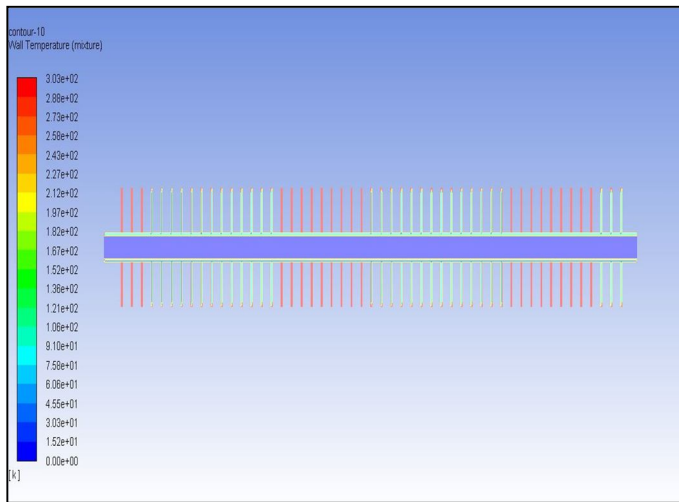


Fig. 26 Wall temperature contour of condenser

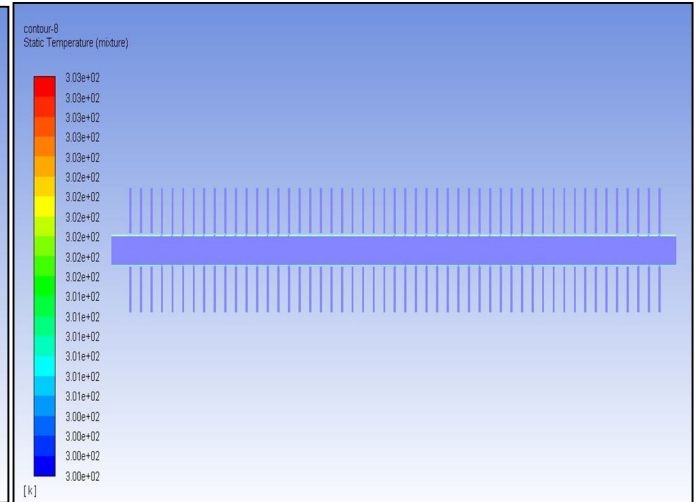


Fig. 27 Static temperature contour of condenser

The wall temperature contour of condenser is depicted above. It can be seen that the wall temperature at the tip is maximum throughout. It can also be seen that the wall temperature changes in accordance with the phase of travel. The static temperature contour of condenser is depicted above.

The static temperature is found to be constant throughout the condenser. It can be inferred that the static temperature is found to be constant irrespective of the phase change.

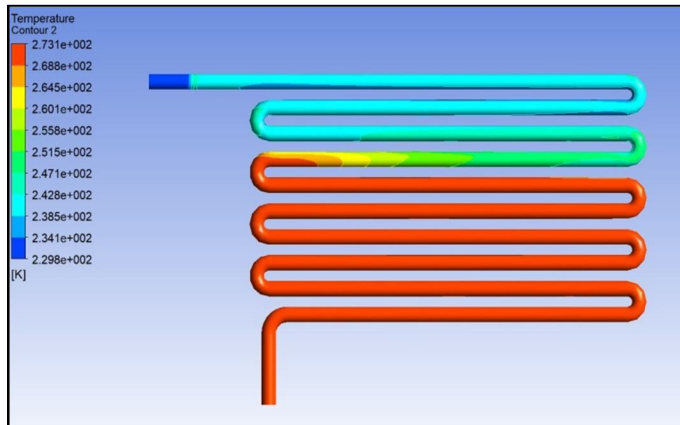


Fig. 28 Temperature contour of evaporator

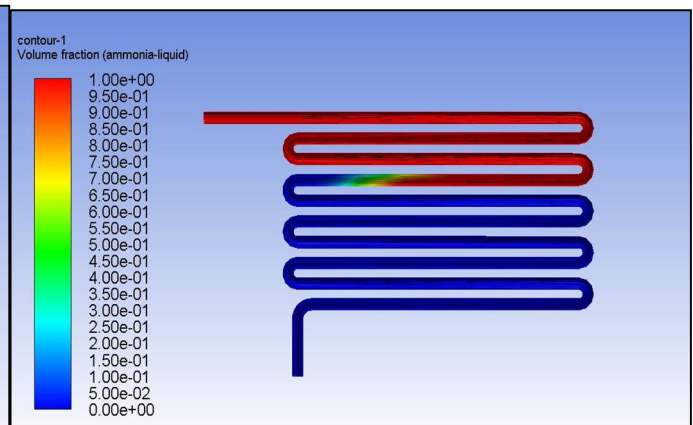


Fig. 29 Volume fraction contour of evaporator

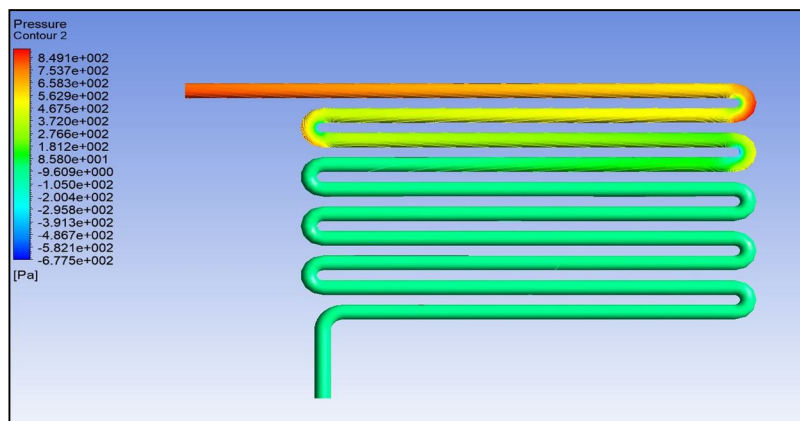


Fig. 30 Pressure contour of evaporator

The temperature, volume fraction and pressure contours of evaporator are depicted above. The temperature is increasing to a larger extent as it passes through the evaporator. The temperature reaches the maximum in a short span as it passes through the evaporator. The volume fraction of ammonia liquid at the inlet is given as 1. The coolant is proportionality used up and it is decreasing as it passes through. The volume fraction is found to be minimum at the exit. The pressure contour of evaporator is depicted above. The pressure within the evaporator is decreasing as it passes through. It is also seen that the pressure concentration is maximum at the bends than in straight directions. A minimum pressure is obtained at the exit.

The multi linear regression analysis indicates that the model's degree of explaining variance in the dependent variables is $R^2 = 98.2\%$ for regression of COP and that for exergetic efficiency was 98.5% . Looking at these coefficients, it can be said that the model predicts the dependent variables very well. Table 3 shows that maximum COP of 0.65 is obtained for $T_c = 35\text{ }^\circ\text{C}$, $T_e = 10\text{ }^\circ\text{C}$, $T_g = 150\text{ }^\circ\text{C}$, $\epsilon_{RHE} = 0.75$, and $\epsilon_{SHE} = 0.75$ and maximum exergetic efficiency is 23.94% for $T_c = 35\text{ }^\circ\text{C}$, $T_e = -5\text{ }^\circ\text{C}$, $T_g = 120\text{ }^\circ\text{C}$, $\epsilon_{RHE} = 0.6$, and $\epsilon_{SHE} = 0.6$ for the Taguchi design.

TABLE VII
Response of SN for COP

Level	T_c ($^\circ\text{C}$)	T_e ($^\circ\text{C}$)	T_g ($^\circ\text{C}$)	ϵ_{RHE}	ϵ_{SHE}
1	-4.896	-7.208	-6.316	-6.051	-6.491
2	-5.506	-6.353	-6.129	-6.084	-6.320
3	-6.400	-5.883	-6.114	-6.129	-5.972
4	-7.830	-5.188	-6.073	-6.368	-5.849
Delta	2.934	2,020	0.243	0.317	0.642
Rank	1	2	5	4	3

TABLE VIII
Response of Means for COP

Level	T_c ($^\circ\text{C}$)	T_e ($^\circ\text{C}$)	T_g ($^\circ\text{C}$)	ϵ_{RHE}	ϵ_{SHE}
1	0.5726	0.4389	0.4841	0.5015	0.4781
2	0.5316	0.4839	0.4984	0.5032	0.4874
3	0.4818	0.5142	0.5027	0.4977	0.5107
4	0.4067	0.5558	0.5075	0.4903	0.5165
Delta	0.1659	0.1169	0.0234	0.0128	0.0384
Rank	1	2	4	5	3

TABLE IX
Response of SN for Exergetic Efficiency

Level	T_c ($^\circ\text{C}$)	T_e ($^\circ\text{C}$)	T_g ($^\circ\text{C}$)	ϵ_{RHE}	ϵ_{SHE}
1	25.35	25.74	24.71	24.12	23.69
2	24.69	24.97	24.29	24.09	23.84
3	23.75	23.50	23.74	24.03	24.20
4	22.23	21.82	23.28	23.79	24.29
Delta	3.11	3.92	1.43	0.34	0.60
Rank	2	1	3	5	4

TABLE X
Response of Means for Exergetic Efficiency

Level	T_c ($^\circ\text{C}$)	T_e ($^\circ\text{C}$)	T_g ($^\circ\text{C}$)	ϵ_{RHE}	ϵ_{SHE}
1	18.95	19.70	17.96	16.57	15.93
2	17.65	17.97	17.07	16.29	16.04
3	15.51	15.12	15.52	16.46	16.48
4	13.06	12.37	14.62	15.85	16.73
Delta	5.89	7.33	3.35	0.72	0.80
Rank	2	1	3	5	4

Table 7 and 8 shows the response of SN ratio and means for COP respectively. From both the tables it can be seen that condenser temperature has maximum influence on COP of all selected parameters.

Table 9 and 10 shows the response of SN ratio and means for exergetic efficiency respectively. It is observed from both the tables that evaporator temperature has maximum influence on exergetic efficiency of all selected parameters.

X. CONCLUSIONS

The absorption refrigeration system chosen here is an established system. In spite of this being well-versed we have taken up this system to pave out ways for future study of ARS and obtain the optimizing parameter for this cycle. We have ammonia + water as the working pair and operated the cycle for various temperature ranges of the evaporator, generator and absorber, we also worked on a number of stages to check the COP of the system. In the process we obtain the optimum parameters for smooth operation of the cycle. Based on the optimum results we made an analysis and made the feasibility study of the cycle. The result obtained is quite encouraging and it shows that using an ARS system instead of VCR, the plant runs in a net profit. The evaporator temperature has a very insignificant effect on the COP of the system and thus does not change the COP even if we increase the temperature. The generator has a very vivid impact on the COP. As we increase the generator temperature the COP value decreases. It further concrete our base for using low grade heat as the source of power for operating the generator because there is no pump and no electrical input for the working of the vapour absorption refrigerator during the day time. During night time there is no availability of solar energy therefore a small electrical heater is attached to the vapour absorption refrigerator. Thus the vapour absorption refrigerator works throughout the day.

XI. NOMENCLATURE

TABLE XI
Symbols, Abbreviations and Nomenclature

SYMBOLS, ABBREVIATIONS AND NOMENCLATURE	CONTENT
Q_a	Heat of Absorption
T_o	Temperature of external heat sink
P_g	Generator pressure
T_g	Generator temperature
Q_g	Heat supply to generator
Q_c	Heat rejected at condenser
P_e	Evaporation pressure
Q_e	Heat supply at evaporator
T_e	Temperature of evaporator
COP	Coefficient of performance
ϵ_{RHE}	Effectiveness of refrigerant heat exchanger
ϵ_{SHE}	Effectiveness of solution heat exchanger
η_{exe}	Exergetic efficiency

XII. ACKNOWLEDGMENT

We thank our Principal Dr.V.Selladurai, M.E., Ph.D., and Professor and Head, Department of Mechanical Engineering Dr.K.Marimuthu, M.E., Ph.D., for their support and for providing us with efficient lab facilities to complete this project successfully.

REFERENCES

- [1] Sen, Nisha and Singh, O. K. (2016) "Study of Vapour Absorption System Using Various Working Fluids." International Journal of Science and Research (IJSR) 5(4):2150–54.
- [2] Ganguly, Sayantan, Date, A. and Akbarzadeh, A. (2019) "On Increasing the Thermal Mass of a Salinity Gradient Solar Pond with External Heat Addition : A Transient Study" Energy 168:43–56.
- [3] Chen, Guangming and Hihara, E. (1999) "A New Absorption Refrigeration Cycle Using Solar Energy." 66(6):479–82.
- [4] Umap, Vrushali, M. and Waghmare, S. (2017) "Studies on Performance of PEMFC." 8(1):1–5. Vol. Solar Energy. 1993. "No Title." 50(5):453–58.
- [5] Wang, Yunfeng, Li, M., Du, W., Ji, X. and Xu, L. (2018) "Experimental Investigation of a Solar-Powered Adsorption Refrigeration System with the Enhancing Desorption." 155(October 2017):253–61.
- [6] Dayal, Sarvesh and Sharma, R. (2018) "Design of Solar Powered Vapour Absorption Refrigeration System 1." 1083–89.
- [7] Adarkar, Lalit, P. and Namdeo, O. R. (2017) "Review of Vapour Absorption System and Vapour Compression System ." 251–55.
- [8] Aprea, C., Greco, A., Habib, K., Abed, A. M. and Sopian, K. "A CASE STUDY OF A LOW POWER VAPOUR." (110).
- [9] Bellos, Evangelos, Ioannis-christos Theodosiou and Vellios, L. (2018) "Investigation of a Novel Solar-Driven Refrigeration System with Ejector." *Thermal Science and Engineering Progress*.
- [10] Elsheikh, Ammar, H., Swellam, W., Abd, M. and Kabeel, A. E. (2019) "Modeling of Solar Energy Systems Using Arti Fi Cial Neural Network : A Comprehensive Review." 180(October 2018):622–39.



- [11] Fellah, Ali, Boukhchana, Y. and Brahim, A. B. (2019) "PT US CR." *International Journal of Refrigeration*.
- [12] Girish K.V.S., Shabari, Praveen, R., Nair, D. and Sahu, D. (2018) "A Case Study on Solar Vapour Absorption Refrigeration System." *International Journal of Engineering & Technology* 7(4.5):44.
- [13] Xu, S. M., Huang, X. D. and Du, R. (2011) "An Investigation of the Solar Powered Absorption Refrigeration System with Advanced Energy Storage Technology." 85:1794–1804.
- [14] Lokesh, Y. (2015) "To Study Solar Vapour Absorption Refrigeration Systems." 2(7):703–12.
- [15] Zeyghami, Mehdi, Goswami, D. Y. and Stefanakos, E. (2015) "A Review of Solar Thermo-Mechanical Refrigeration and Cooling Methods." *Renewable and Sustainable Energy Reviews* 51:1428–45.



10.22214/IJRASET



45.98



IMPACT FACTOR:
7.129



IMPACT FACTOR:
7.429



INTERNATIONAL JOURNAL FOR RESEARCH

IN APPLIED SCIENCE & ENGINEERING TECHNOLOGY

Call : 08813907089  (24*7 Support on Whatsapp)